Results from a First Prototype of a Compton Prostate Probe

C. Lacasta[1], J. Bernabeu[1], D. Burdette[4], E. Chesi[4,5], N. H. Clinthorne[2], Y. K. Dewaraja[2], K. Honscheid[4], H. Kagan[4], G. Llosá[1], M. Mikuž[3], P. Modesto[1], W. L. Rogers[2], A. Studen[3], P. Weilhammer[5,6], L. Zhang[2], D. Zontar[3]

[1]IFIC, CSIC-UVEG, Valencia, Spain
[2] Radiology Dpt, University of Michigan, Ann Arbor, Michigan, USA
[3]Physics Dept., Jožef Stefan Institut, Ljubliana, Slovenia
[4]Physics Dept., Ohio State University, Columbus, Ohio, USA
[5]CERN, Geneva, Switzerland
[6]Universita degli Studi di Perugia, INFN, Perugia, Italy

***Abstract*— A first prototype of a Compton prostate probe has been built using a stack of five 4×1 cm^2, 1 mm thick silicon pad detectors as a scatter detector, surrounded by three scintillation detectors in which the absorption of the scattered photons takes place. The silicon pad dimensions are 1.4×1.4 mm^2 which provide the required spatial resolution. The energy resolution in the silicon sensors is about 1.4 keV FWHM as determined from several gamma sources. The results obtained validate the simulation predictions that foresee an improvement over current SPECT techniques by a factor 16-40 in sensitivity and 4-5 in spatial resolution simultaneously for an intra-rectal probe built employing this concept and placed at 2 cm from the prostate.**

I. Introduction

PROSTATE cancer is the second most common cause of cancer-related deaths in men and the lifetime risk of being diagnosed with prostate cancer is 1 in 14. As a result, the development of applications that are able to measure the local extent of the disease, provide improved guided biopsy, staging or identification of aggressive cancers, together with the measurements of early biological effects of therapy, are of outstanding importance. Among them, radiotracer techniques offer one of the best ways. Current state-of-the-art devices, like SPECT and PET, are not adequate. SPECT, for instance, suffers from poor resolution and low counting rate and, in addition, both resolution and sensitivity are coupled due to the mechanical collimators. The resolution for PET, on the other hand, is somewhat better, but it suffers from the strong attenuation in the pelvic region, since it needs to detect the two photons in coincidence.

An intra-rectal probe based on the principle of the Compton-scatter camera can, under the appropriate conditions, outperform those devices by as much as a factor 4-5 in spatial resolution and, in sensitivity, by a factor as high as 40. Furthermore, it is useful over a wide range of radioisotopes and, most important, its performance improves with radioisotope energies.

Carlos.Lacasta@ific.uv.es

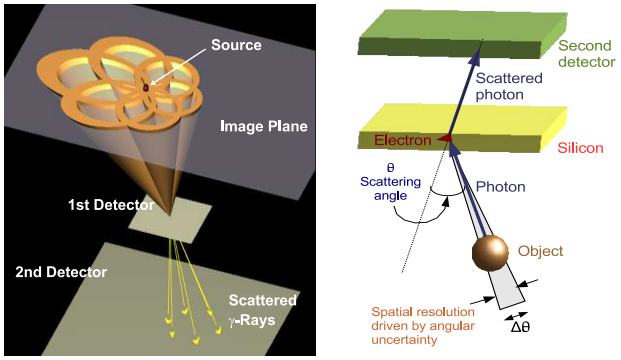

Fig. 1. Right: Compton camera concept. A photon from the source Compton scatters is the silicon sensor and the scattered photon is absorbed in a second detector. From Compton kinematics the scattering angle can be calculated. Left: Cones defined by the position and energy measurements.

II. The Compton Camera Concept

The Compton Camera proposes electronic collimation instead of mechanical collimation. As a consequence resolution and efficiency are not coupled anymore and both can improve simultaneously. The principle, depicted in Fig.1, is to scatter via the Compton effect the initial photon in a finely segmented silicon sensor and measure the scattered photon in a second detector which could be an advanced camera head developed for SPECT. The quantities to be measured are, thus, position and energy deposition in both detectors.

For each detected photon the source can be anywhere on the surface of a cone. The opening angle is the scattering angle and the axis is defined by the interaction points as measured in both detectors. The intersection of many of those cones will define the source position.

The resolution of the scattering angle depends, mainly, on the energy resolution in the scatter detector and on the energy of the incoming photon. There is, however, a inherent physical limit on the angle resolution given by the Doppler broadening effect in the scattering process, the magnitude of which depends on the detector material and the energy of the original photon.

This is shown in Fig. 2 where the solid lines represent

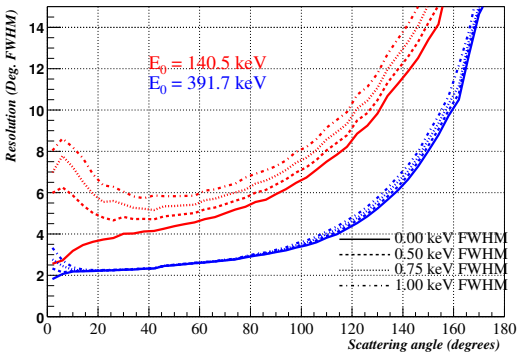

Fig. 2. Angle resolution in degrees FWHM as a function of the scattering angle

the minimum attainable resolution due to Doppler broadening and the dashed curves show the contribution of different levels of uncertainty in the energy in the scatter detector. One may conclude that small angles ($>20^o$) are favored and the performance certainly improves with the photon energy, making the relative contribution of both Doppler broadening and energy resolution much smaller. The best angle resolution is obtained for angles ranging from 20^oo to about 90^o. At 140 keV this range corresponds to an energy range, in the scatter detector, of 5-30 keV, which somehow defines the lower limit on the energy threshold to the recoil electron.

III. The prostate probe

Our proposal for a prostate probe is shown pictorially in Fig. 3. It consists of a stack of packed silicon sensors that would allow to be as close as 1 cm to the prostate. The second detector would be external and could be, in principle, a conventional SPECT device. The main issues of the scatter detector are the packaging, to make it as small as possible, heat removal to minimize electronics noise and the fact that there is material between both detectors which will, certainly, affect the performance.

Detailed simulations have been made in the past [1], taking into account the background from the nearby organs and the attenuation in 10 cm tissue and the results are quite compelling, suggesting that there could be a gain of a factor 5 in resolution and a factor up to 40 in the sensitivity compared with existing SPECT devices optimized either for resolution or sensitivity.

IV. The prototype

We have built a first prototype of a demonstrator[6][5]. It consists of a stack of five silicon pad detectors manufactured by SINTEF [4]. The pad size is 1.4×1.4 mm^2 and there are 256 of them readout by 2 VATAGP3 self-triggering chips with 128 channels each. As second detector we used 3 NaI camera heads that we took from an existing system [3]. All the detectors were mounted on a precision mechanical support. We used a VME based, customized data acquisition system.

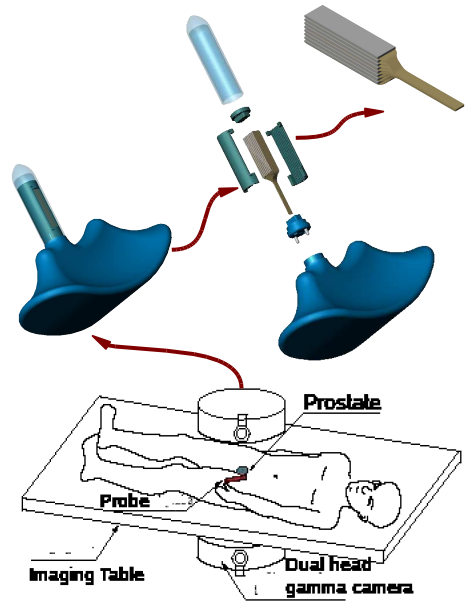

Fig. 3. A possible realization of an intra-rectal prostate probe. The core of the device is a stack of densely packed silicon sensors where the incoming photon will Compton scatter.

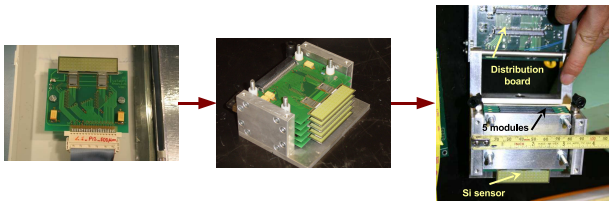

Fig. 4. Left: A module containing the silicon sensor and the associated readout electronics. Center: A stack of silicon modules. Right: The silicon stack connected to a distribution borad that presents the devide to the DAQ system as a single object.

A. The silicon module

The silicon sensors and the readout ASICs were assembled together in a PCB board. Five of those modules were stacked together to form the scatter detector. They were packed into a dense mechanical assembly with a separation of about 5 mm between them. The modules, in turn, are connected to a distribution board and presented to the data acquisition system as a single object.

The energy resolution measured for the modules when operated individually was 1.4 keV FWHM and 1.5 keV FWHM when operated together. The five modules could be operated with a threshold of 15 keV for the self–triggering ASICs.

B. Scintillation detectors

The second detector consisted of three scintillation heads taken from CSPRINT [3]. There was no particular reason for choosing them other than availability. The crystals were 1.27 cm thick, readout by 20 PMTs, yielding a spatial resolution of 2 mm RMS and an energy resolution of 4-8% RMS. It provided a trigger on the hardware energy sum, which in coincidence with the silicon ASICs trigger was giving the system trigger.

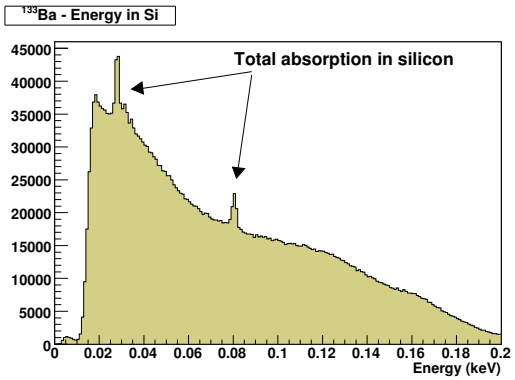

Fig. 5. ^{133}Ba energy spectrum as measured by the silicon sensors when operated in coincidence with the scintillators. One can observe the X–ray peak at 30 keV and the gamma peak at 80 keV which correspond to total absorption in the silicon. This gives an idea of the amount of accidental coincidences in our system.

C. Timing

The system trigger was built by the coincidence of the scintillation and the silicon detector triggers. The timewalk of the VATAGP3 chips produced long tails at low values of the coincidence time. In future, this will be avoided by using ASICs with built–in timewalk compensation. This, together with the poor count rate performance of the scintillation detectors forced us to operate with a coincidence window of 200 ns. As a result the number of accidental coincidences was quite high (see Fig.5) and we had to avoid direct incidence of the source photons into the scintillators by placing them in a plane orthogonal to the source –one at each side of the silicon sensors and the third one below– ending up in a range of scattering angles (about 90^o) at the edge of the optimum shown in Fig.2.

V. The Data Set

The main goals of this work were to study the effects of the geometry and the incoming photon energy on the final performance of the system. To this end, the distance from the scatter detector and the scintillators was varied and data was taken with 3 different values: D0(10 cm), D05(D0+5 cm) and D10(D0+10 cm). To study the effect of the photon energy on the system performance we took data from 2 different sources: ^{56}Co (122 keV) and ^{133}Ba (272, 302 and 356 keV).

For the reconstruction we used a *Compton optimized* list-mode MLEM method[2]. Only events with a single interaction in the silicon and in the scintillators were used for the reconstruction.

The main problems when analyzing the data were, first that the scattering angle range was not optimal nor equal in the different geometries. In order to be able to compare, we restricted the data to be between 60^o and 70^o for all data sets. Second, the energy resolution of the scintillators was not good enough to separate the ^{133}Ba peaks. To resolve them, we used the prior knowledge of where the source was to calculate the *real* scattering angle and, together with energy measured in the silicon, obtain an estimate, E_0 of the total energy by using

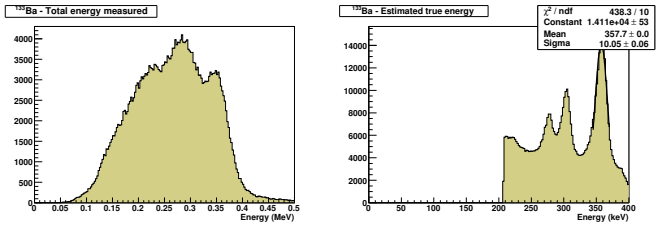

Fig. 6. Right: Distribution of the the photon energy as measured in out system. The performance of the scintillators is too poor to resolve the ^{133} peaks. Left: Total energy estimated when using the known source position, the interaction positions measured by the system and the energy measured in the silicon. It corresponds to E_0 in (1)

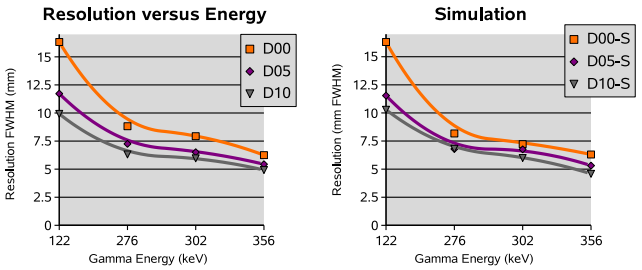

Fig. 7. Left: data from table I shown graphically. The abscissa is the photon energy and each of the curves represents one geometry configuration. Right:Spatial resolution obtained after simulating our setup. If compared with the data, one can see that the agreement is quite good.

Compton kinematics. The ^{133}Ba peak selected was the one maximizing equation (1).

$$P(E_{peak}|E_0) \approx P(E_0|E_{peak})P(E_{peak}) \quad (1)$$

$P(E_0|E_{peak})$ is the probability of obtaining E_0 when the ^{133}Ba peak is E_{peak} and is given by the distributions in Fig.6 right. $P(E_{peak})$ is simply the probability that the source emits a photon with that energy.

VI. Results

As mentioned in section IV-C the source had to be placed further away than desired. The distance between the source and the scatter detector was 11.3 cm. The results will be affected by that since the demonstrator could not operate close to the source.

The results are summarized in table I and pictorially in Fig. 7 left. The resolution improves with the distance between the first and second detector. This is easy to understand since for increasing distances the contribution of the spatial resolution in the scintillators is smaller. Also, the impact is

TABLE I

Spatial resolution in mm FWHM for different geometries and incoming photon energies as obtained from the data.

Energy (keV)	D00	D05	D10
122	16.3	11.7	9.9
276	8.8	7.2	6.3
302	7.9	6.5	6.0
356	6.2	5.4	4.9

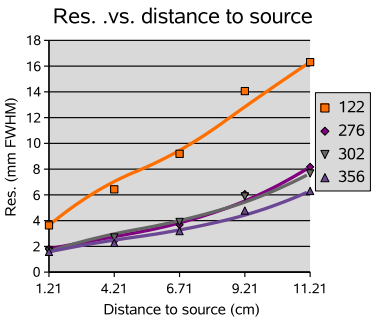

Fig. 8. Extrapolation of the resolution to smaller distances between the scatter detector and the source as obtained from the simulated data.

higher for low energy photons, as expected from Fig.2. The effect of the photon energy is clearly visible and there is almost a factor 2 improvement when going from 122 keV to 356 keV.

From the data it is clear that resolutions of order 5 mm FWHM can be obtained with 356 keV photons, while for an energy of 122 keV the resolution is about 10 mm FWHM. Considering that the distance between the scatter detector and the source was about 11 cm, the results are quite good compared with resolutions of order 10 mm FWHM obtained at 141 keV with conventional SPECT located 10 cm away from the source.

Fig. 7 right shows the resolutions obtained after simulating our setup with Geant4 [7]. The results agree perfectly with the data. That gives us enough confidence in our simulation to try and extrapolate the system behavior to smaller distances between the source and the scatter detector. Results from this calculations are shown in Fig. 8 for the worst case geometry, D00. According to this, one could expect resolutions below 4 mm FWHM already at low energies –with an optimized geometry– and a factor 2 smaller, that is, 2 mm FWHM for higher energy gammas.

VII. Conclusion

To conclude, the first steps in building a real prototype of a Compton prostate probe have been taken by making a stack of five 1 mm thick silicon sensors that have been operated reliably in coincidence with a scintillator head.

The effects of geometry and photon energy on performance have been evaluated and, for a more optimized geometry, one can obtain spatial resolutions of 10 mm FWHM with a 122 keV photon and a factor two better, that is, 5 mm for a 356 keV photon with a point source located at 11 cm from the scatter detector. According to our simulation, a resolution of a factor 2 better can be obtained, that is 4 mm FWHM for 122 keV photons and 2 mm FWHM for 356 keV photons when the source is located at 1 cm from the scatter detector.

There are some issues to improve, like the timewalk in the silicon readout ASICs' comparators, the system stability to further reduce the trigger threshold in the silicon sensors and operate with a scintillator with a better count rate and energy resolution performance. This is being addressed at the moment and the next generation of silicon readout ASICs will incorporate a faster comparator stage and a built–in timewalk compensation mechanism. Also a new fast scintillator camera head will be used in the next demonstrator. Further tests should demonstrate the performance with extended sources and near field operation.

References

[1] L. Zhang, S.J. Wilderman, N.H. Clinthorne, W.L. Rogers. IEEE Nuc. Sci. Vol. 3, p. 20/119-22, 2001
[2] S.J. Wilderman, N.H. Clinthorne et al, IEEE Nuclear Science Symposium and Medical Imaging Conference, Vol 3, 1999, p.1716.
[3] W.L. Rogers, N.H. Clinthorne, L.Shao et al, *IEEE Trans. Med. Im.* 7: 291-297 (1988).
[4] D. Meier et al., IEEE Trans. Nucl. Sci. 49, 812-816, 2002
A. Studen et al., Nucl. Instrum. Meth. A501, 273-279, 2003
[5] G. Llosá et. al. *Nuc. Ins. Meth. A* Vol 527, 58-61 (2004)
[6] A. Studen et al. *Nuc. Ins. Meth. A* Vol 531, 258-264 (2004)
[7] S. Agostinelli et al., *Nuc. Ins. Meth. A* Vol 506 (2003), 250-303